

1           **Quantifying Antarctic Bottom Water and North**

2                           **Atlantic Deep Water Volumes**

3  
4                           **Gregory C. Johnson<sup>1,2</sup>**

5  
6                           *For Journal of Geophysical Research, Oceans*

7  
8                           Submitted: 2 August 2007

9                           First Revision: 30 October 2007

10                          Second Revision: 9 January 2008

11                          Running Title: Quantifying AABW and NADW Volumes

12  
  

---

  
<sup>1</sup> NOAA/Pacific Marine Environmental Laboratory, 7600 Sand Point Way Bldg. 3,  
Seattle Washington 98115-6349, U.S.A.

<sup>2</sup> Corresponding author. Tel.: +1-206-526-6806; fax: +1-206-526-6744, E-mail  
address: gregory.c.johnson@noaa.gov (G. C. Johnson).

12 *Abstract.* A near-global census of Antarctic Bottom Water (AABW) and North Atlantic  
13 Deep Water (NADW) is essayed through a non-negative least-squares analysis of  
14 conservative and quasi-conservative seawater properties. AABW thickness generally  
15 decreases from south to north, modulated by ocean bathymetry. Likewise, NADW  
16 thickness generally decreases from north to south in the Atlantic Ocean. NADW  
17 dominates below the thermocline of the Atlantic Oceans at least as far south as the  
18 subtropical gyre of the South Atlantic Ocean, with a lesser, but still significant, influence  
19 around the entire Antarctic Circumpolar Current, in the Indian Ocean, and in the Pacific  
20 Ocean. However, in the Pacific and Indian Oceans AABW dominates below the  
21 thermocline. In addition, measurable quantities of AABW reach into the abyssal North  
22 Atlantic on both sides of the mid-Atlantic Ridge. The census results suggest that AABW  
23 occupies roughly twice the volume of NADW in the three main oceans, and that AABW  
24 is in contact with roughly twice the area of the deep main ocean floor compared with  
25 NADW. However, these results are somewhat sensitive to choices of water masses, their  
26 values of seawater properties, and the weightings of the seawater properties used in the  
27 analysis.

28 *Index Terms.* 4283 Water masses; 4536 Hydrography and tracers; 4532 General  
29 Circulation; 4211 Benthic boundary layers; 4215 Climate and interannual variability

30 *Keywords.* Antarctic Bottom Water; North Atlantic Deep Water; Deep Ocean Ventilation

## 1. Introduction

Bottom waters formed around Antarctica are often referred to collectively as Antarctic Bottom Water (AABW). Several varieties of AABW are produced and exported around the continental margins of Antarctica, including Weddell Sea Bottom Water (WSBW), Ross Sea Bottom Water (RSBW), and Adélie Land Bottom Water (ALBW) [Warren, 1981; Orsi *et al.*, 1999]. The formation process for AABW is complex [Foster and Carmack, 1976], but certainly involves, among other processes, entrainment of ambient waters by dense shelf waters as they move down the continental slopes into the abyss. The different AABW varieties have varying characteristics [Orsi *et al.*, 1999], all of which contribute to the densest waters in the main basins of the global ocean. All varieties of AABW are very cold and relatively fresh in comparison to North Atlantic Deep Water (NADW). AABW has been shown to spread northward to cover much of the world ocean floor, with the exception of the Arctic and some of the North Atlantic Ocean, where NADW overlies the ocean bottom [Mantyla and Reid, 1983; Orsi *et al.*, 2001]. AABW gradually warms by mixing with lighter overlying waters as it spreads northward into deep basins, often with more abrupt seawater property changes at sills between basins.

Dense overflows of waters formed in the Greenland, Iceland, and Norwegian Seas flow southward into the North Atlantic through various gaps between Greenland, Iceland, the Faeroe Islands, and Scotland [Dickson and Brown, 1994]. As these overflow waters descend into the abyssal North Atlantic, they also mix with ambient waters. While these overflow waters comprise the densest waters in some of the North Atlantic and thus sink to the sea floor near where they are formed. They are substantially warmer, saltier, and

54 lighter than AABW. These northern overflow waters are overlain and augmented by a  
55 somewhat warmer and lighter water mass, Labrador Sea Water (LSW), that forms as it is  
56 directly ventilated during wintertime by deep convection in the Labrador and Irminger  
57 Seas [*Talley and McCartney*, 1982]. Together the northern overflow waters and the  
58 overlying LSW are often referred to as NADW. The relatively warm and salty signature  
59 of NADW has been traced southward to the Antarctic Circumpolar Current (ACC),  
60 where it flows eastward, with some northward spreading into the Indian and Pacific  
61 Oceans [*Reid and Lynn*, 1971].

62       Here the spatial distributions and volumes of AABW and NADW in the global  
63 oceans are quantified and discussed using a non-negative least-squares analysis of  
64 conservative and quasi-conservative gridded seawater properties available in a global  
65 hydrographic climatology [*Gouretski and Koltermann*, 2004]. The analysis takes  
66 inspiration from Optimum MultiParameter (OMP) analysis [*Tomczak and Large*, 1989],  
67 but differs in some details. The data set and the seawater properties used are described in  
68 Section 2. The analysis procedures, and some of the ways they differ from OMP, are  
69 presented in Section 3. The choices of water masses are reasoned and the estimation of  
70 their seawater properties for the analysis is described in Section 4. The results of the  
71 analysis are set forth in Section 5 using vertical sections of water-mass concentrations,  
72 maps of depth-integrated and bottom water mass concentrations, and global average  
73 volumes of water masses. Sensitivities of the results to different choices of AABW  
74 seawater properties, LSW seawater properties, and model weights are explored in Section  
75 6. The possible impacts of different water mass choices, the implications of the results

for NADW and AABW residence times and diffusivities, and the potential ramifications of time variability are discussed in Section 7.

## 2. Data

The data used here are from the WOCE Global Hydrographic Climatology [Gouretski and Koltermann, 2004], including temperature (T), salinity (S), and concentrations of dissolved oxygen ( $O_2$ ), nitrate ( $NO_3$ ), phosphate ( $PO_4$ ), and silicic acid ( $H_4SiO_4$ ). The climatology was produced by objectively mapping seawater properties on isopycnal surfaces onto a grid with  $0.5^\circ$ -spacing in latitude and longitude and 45 depth levels from the surface to 6000 m. Depth intervals increase from 10 m above 50 m to 250 m below 1500 m.

All these seawater properties are used here, but with some modification. Pressure (P) is calculated from depth and latitude, and potential temperature ( $\theta$ ) and potential density anomaly ( $\sigma_\theta$ ) referenced to the surface are calculated from S, T, and P, as is the planetary component of potential vorticity ( $PV = f/\rho \partial\rho/\partial z$ ) where  $f$  is the local Coriolis Parameter, and  $\rho$  is the potential density referenced to the central pressure over which its derivative with respect to depth,  $z$ , is being calculated. Planetary potential vorticity is a conservative quantity for large-scale ocean circulation in the absence of mixing [Pedlosky, 1987]. Values of  $O_2$ , reported in ml/l, are converted to  $\mu\text{mol/kg}$  by multiplying by a conversion factor of  $44.66 \mu\text{mol/ml}$  and dividing by  $1 + 0.001\sigma_\theta$  (with units of kg/l).

Nutrient data are combined with oxygen data using global average deep Redfield ratios to construct quasi-conserved seawater properties. The largely conservative

quantities PO and NO [Broecker, 1974] are calculated by combining phosphate and nitrate concentrations with dissolved oxygen concentrations. Deep Redfield ratios [Anderson and Sarmiento, 1994] are used so  $PO = 170[PO_4] + [O_2]$  and  $NO = 10.625[NO_3] + [O_2]$ . NO and PO should contain some independent information as a result of large-scale variations in deep Redfield ratios. A quantity referred to here as deep SO  $= 1.66[H_4SiO_4] + [O_2]$  is also calculated [Poole and Tomczak, 1999] using a global average ratio of deep  $NO_3$  to  $H_4SiO_4$  values of 1 to 6.4 [Sarmiento et al., 2007] along with the other deep Redfield ratios. The deep ratios of  $NO_3$  to  $H_4SiO_4$  do vary significantly from ocean to ocean [Sarmiento et al., 2007], so deep SO, while it should also contain some independent information from NO and PO, is also likely less conservative than either of these two tracers. However, deep SO is still closer to being conservative in deep waters than silicic acid alone would be.

### 3. Analysis procedure

This study focuses on quantification of global distributions of AABW and NADW using seawater properties. An analysis taking substantial inspiration from Optimum MultiParameter (OMP) is used for this purpose. OMP is a weighted, multi-parameter, least-squares mixing model with a non-negativity constraint [Tomczak and Large, 1989]. The model allows quantification of the relative amounts of water-masses assuming each water mass can be described by a set of conserved seawater properties and that mass is conserved. Here six conservative, or quasi-conservative seawater properties (S,  $\theta$ , PV, PO, NO, and deep SO) are used in the analysis. With these six properties and the additional constraint of mass conservation, seven water masses can be (and are) defined, each with specific properties determined from observations. Using seven water masses

with seven constraints means that the solution would be evenly determined, and not over determined, except that the non-negativity constraint provides one more constraint on the solution. Nonetheless, estimating seven water mass concentrations from six seawater properties is not standard practice for OMP, and may strain the limits of the analysis.

Within the framework of OMP, weights are selected to determine the relative importance of mass conservation and the various seawater properties in the solution [Tomczak and Large, 1989]. Here, for each property, the mean and standard deviation of the values for all seven water masses being studied is estimated. The model and data are then normalized by these parameters. This weighting alone would ensure that all properties and mass conservation would have about an equal influence on the solution.

However, further choices can be (and are here) made as to the relative influence of each seawater property used and the additional constraint of mass conservation on the solution. Here  $S$  retains the normalized variance of unity. Since  $S$  and  $\theta$  are conserved, they are given roughly equal weight by scaling  $\theta$  so that its variance is equal to that of  $S$  in terms of their relative contribution to density changes (assuming a ratio of thermal expansion to haline contraction,  $\alpha/\beta = 0.25$ , typical of deep waters). With the possible exception of this choice, the weights selected are subjective. PO and NO, being quasi-conserved but somewhat noisier than  $S$  or  $\theta$ , are assigned a variance of 0.5 of that of  $S$ . This means that together they have an effect on the solution roughly equal to that of  $S$ . Deep SO, which is probably less well conserved than PO and NO, is assigned a variance of 0.25 that of  $S$ , meaning that it has roughly half the impact of either PO or NO on the solution. PV is also assigned a variance of 0.25 that of  $S$  because, while conservative, it is estimated from a vertical derivative of density, and is thus significantly noisier than  $S$  or

144  $\theta$ . Mass conservation is given the largest large weight, with a variance equal to the sum  
145 of that of the six water properties used. Thus mass conservation is as important to the  
146 solution as all the other seawater properties combined. The sensitivity of the results to  
147 variations in these weightings is explored in Section 6. Again, these weighting choices  
148 differ from those used in OMP.

149 With the seawater properties characterizing each water mass chosen, and the  
150 weights specified, the model is inverted and applied to the data to find a solution for the  
151 relative fractions of each water mass. A non-negative least-squares minimization is used,  
152 so that negative fractions are not allowed.

153 The final step is to examine the solution, and determine where it is valid. Two  
154 parameters are used to quantify solution validity. Where either the squared norm of the  
155 residuals exceeds 0.25 or the sum of all seven water-mass fractions differs by more than  
156 0.05 from unity, the results are deemed invalid and water-mass fractions there are set to  
157 zero. Most of the waters below the permanent pycnocline in all the main ocean basins  
158 have valid solutions by these criteria, and most upper ocean waters are excluded. The  
159 maximum pressures above which results are deemed invalid range from as little as 100  
160 dbar in the parts of the subpolar regions to as much as 1200 dbar (although usually  
161 shallower) in the bowls of the subtropical thermoclines. Tropical regions have solutions  
162 generally valid below 400 – 600 dbar, except for in the oxygen-poor regions in the  
163 eastern tropical Atlantic and eastern tropical Pacific, where solutions as deep as 700 and  
164 1000 dbar, respectively, are excluded, probably because of denitrification or deep vertical  
165 mixing.

#### 4. Water-masses and their seawater properties

Seawater properties are estimated for seven prominent bottom, deep, and intermediate water masses (Table 1), and for one sensitivity experiment, a surface water mass. While seven water masses are inadequate to characterize fully the properties of the global ocean below the permanent pycnocline, those used here are selected with the purpose of being representative of the major influences on sub-thermocline water properties outside of the Arctic Ocean and the marginal seas.

Seawater properties of these water masses are estimated based on climatological data within  $5^\circ$  ellipses (in latitude and longitude) at select locations (Figure 1; Tables 2 and 3). The first seven water masses listed (above the upper dividing line in all Tables and black ellipses in Figure 1) are used in the main experiment. The seawater properties for the next three water masses (between the upper and lower dividing lines in all Tables and gray ellipses in Figure 1) are substituted for AABW in a set of sensitivity experiments discussed in Section 6. Finally, the last water mass listed (below the lower dividing line in all Tables), which is derived partly from the climatology and partly from water properties in the literature, is substituted for UNADW in another sensitivity experiment in Section 6. A careful visual inspection of the estimated water-mass fractions for the seven water masses used and the two statistical indicators discussed above (not shown) suggests that below the permanent pycnocline in the main ocean basins, these water masses chosen do a pretty good job of spanning the seawater property space.

Locations where seawater properties are determined are chosen to be near extrema in various properties for these water masses, while being sufficiently removed from

actual overflow regions (where overflow waters contribute to a given water mass). The intent (except for the single near-surface water mass used in one sensitivity experiment) is that the properties will be typical of the water mass after its components have experienced the bulk of any entrainment along its path from a marginal sea or shelf into the ocean interior. Water masses are discussed here from the densest to the lightest.

Seawater properties of the WSBW, here selected for the coldest, densest water found in the climatology over the Weddell Abyssal Plain (Figure 1; Tables 2 and 3) are those used to characterize AABW in most of the results presented here. While this water mass does not escape the Weddell Sea without mixing with the water masses above it [Orsi *et al.*, 1999], it is representative of some of the most extreme AABW seawater properties. It is extremely cold, fresh, with fairly small negative PV values, and large NO, PO, and SO. The sensitivity of the results to different choices for AABW properties is discussed in Section 6.

Seawater properties for two end-members typical of dense (Lower NADW; LNADW) and light (Upper NADW; UNADW) components of NADW are estimated near the center of the Labrador Sea (Figure 1; Tables 2 and 3) to characterize this complex water mass, which has many different components and significant temporal variability [Yashayaev, 2007]. LNADW properties are typical of those of Iceland-Scotland Overflow Water (ISOW) in the region and the UNADW properties estimated in the same location on a lighter horizon (Figure 1; Tables 2 and 3) are typical of a relatively warm, salty, strongly stratified LSW. In Section 6, the colder, fresher, less stratified 1994 values of S,  $\theta$ , and PV for LSW [Yashayaev, 2007] are substituted for those of UNADW from the climatology to explore the sensitivity of the solution to

212 variation in LSW properties. The Denmark Strait Overflow Water (DSOW), sandwiched  
213 between ISOW and LSW, is not explicitly represented. DSOW is a bit warm, salty, and  
214 low in NO, PO, and deep SO than of a mixture of UNADW and LNADW having the  
215 same density. However, in comparison to the property differences between AABW and  
216 LNADW or UNADW, these deviations from a linear mixing model are quite small. On  
217 the whole NADW is relatively warm, salty, and low in NO, PO, and deep SO compared  
218 with AABW (Table 3), with fairly small positive PV values.

219 Mediterranean Sea Overflow Water (MSOW) is introduced from the Mediterranean  
220 Sea into the North Atlantic Basin [*Harvey and Arhan, 1988; Tsuchiya et al., 1992*], but  
221 contrasts quite strongly with UNADW. MSOW is often characterized in the North  
222 Atlantic by a salinity maximum located near 1200 dbar. Here seawater properties for  
223 MSOW are selected on a density horizon where that salinity maximum is strongest in the  
224 open ocean off the coast of Portugal (Figure 1; Tables 2 and 3). As well as being salty,  
225 MSOW is very warm for this density horizon, with high positive PV values, and quite  
226 low in NO, PO, and deep SO.

227 Red Sea Overflow Water (RSOW) is introduced from the Red Sea to the  
228 northwestern Indian Ocean and spreads throughout the Indian Ocean [*Beal et al., 2000*].  
229 Here seawater properties for RSOW are selected at the density of the salinity maximum  
230 in the open Arabian Sea just outside of the Gulf of Aden (Figure 1; Tables 2 and 3). For  
231 this density horizon, RSOW is warm and salty, much like MSOW, another product of an  
232 evaporative basin. In addition, RSOW has intermediate positive PV, and values of NO,  
233 PO, and deep SO that are low for this isopycnal.

Antarctic Intermediate Water (AAIW) is a circumpolar water mass that ventilates the base of the permanent pycnocline. It has a relatively strong expression in the southeast Pacific Ocean, just north of the ACC, where it is coincident with the surface-ventilated Subantarctic Mode Water [McCartney, 1977]. A local vertical salinity minimum is often used to characterize AAIW. Here median values of seawater property data deeper than 400 m on an isopycnal characteristic of that salinity minimum in the Southeast Pacific (Figure 1; Tables 2 and 3) are used to characterize AAIW. On this isopycnal AAIW is cold and fresh, with relatively large negative PV values. In addition, AAIW has high values of NO, PO, and deep SO.

The North Pacific Ocean is locally ventilated only as deep as the North Pacific Intermediate Water (NPIW), often characterized by a salinity minimum near  $\sigma_\theta = 26.8 \text{ kg m}^{-3}$  that is strongest in the Northwest Pacific Ocean [Talley, 1993]. Again, median values of seawater property data deeper than 400 m in the northwest Pacific on that isopycnal are used for this water mass (Figure 1; Tables 2 and 3). NPIW is relatively cold and fresh, with large positive PV values (the largest used here). In addition, NPIW has intermediate values of NO, PO, and deep SO.

## 5. Results

Vertical sections, vertical integrals, volume integrals, and bottom concentrations of water-mass fractions are discussed to quantify the relative roles of the deep North Atlantic and Antarctic water masses in populating the abyss. The sum of LNADW and UNADW is presented here, and is referred to as NADW hereafter. The sole deep Antarctic water mass considered here is AABW, in this section represented by WSBW

(Tables 2 and 3). Vertical sections of fractions of the other water masses (NPIW, AAIW, RSOW, and MSOW) are presented in the auxiliary material.

Fractions of NADW and AABW (Figure 2) along a quasi-meridional section that runs through the deeper portions of the western basins of the Atlantic Ocean (Figure 1) illustrate the relative contributions of North Atlantic and Antarctic influences on the deep waters in this region. The fraction of NADW is above 0.9 throughout much of the deep water column north of about 35°N, and nearly the entire water column in the Labrador Sea. Screening of the water column where residuals are large appropriately removes some North Atlantic thermocline waters from the estimate. The quarantined area forms a bowl reminiscent of the subtropical gyre north of about 10°N and shallower than 900 m at its deepest point. From about 35°N to 50°S, the maximum fraction of NADW is found between 2000 and 4000 m, decreasing from about 0.9 to about 0.4. South of about 50°S, the NADW maximum fraction shoals to about 60°S, where its core reaches a depth near 1000 m and fades to values below 0.2. In contrast, AABW fraction is above 0.9 in the deeper portions of the Weddell Sea, where its seawater properties are selected. In this section the AABW fraction is always bottom intensified, exceeding 0.8 in the Argentine Basin, 0.6 in the Brazil Basin, but only 0.2 north of the equator, and fading to below 0.1 north of about 35°N.

Fractions of NADW and AABW (Figure 3) along a quasi-meridional section that runs through the deeper portions of the western basins of the Indian Ocean (Figure 1) illustrate the dominant role of Antarctic relative to North Atlantic influences in filling the abyss of that ocean. Except for small isolated blobs at the north of the section and near 30°S, the NADW fraction exceeds 0.2 only south of 40°S, and 0.4 only in the core of the

ACC, again tilted up to the south, following isopycnals. North of 40°S, values of NADW generally vary around 0.1 below 2000 dbar. The patchiness of the solution in this region gives some indication of the noise levels in the water mass concentration estimates, resulting from some combination of errors in the climatology and inadequacies in the analysis technique. In contrast with NADW, AABW fills much of the deep Indian Ocean, with bottom fractions exceeding 0.7 in the south until just north of the equator and 0.5 all the way to the northern end of the deep Arabian Sea.

Fractions of NADW and AABW (Figure 4) along a quasi-meridional section that runs through the deeper portions of the central Basins of the Pacific Ocean (Figure 1) illustrate the dominant role of Antarctic relative to North Atlantic influences in filling the abyss of that ocean. The NADW fraction in the Pacific ACC only exceeds 0.3, and thus is weaker than in the Indian Ocean section discussed. A mid-depth maximum exceeding 0.2 is visible in the western Pacific almost as far north as the latitude of the Samoan Passage (~10°S), but this feature vanishes to the north. North of 10°S, NADW fraction below 1000 dbar is generally around 0.1, with some isolated blobs at the northern end of the section exceeding 0.2. As in the western Indian Ocean, AABW fills much of the deep Pacific, with bottom fractions exceeding 0.7 in the south until just north of the equator and 0.6 all the way to the Aleutian Islands.

Depth-integrating the fractions of AABW and NADW at each point in the globe (Figure 5) allows a near-global assessment of the relative roles of AABW and NADW in filling the deep oceans. This depth integral of a water-mass fraction is here referred to as an equivalent thickness. The expressions of mid-ocean ridges are prominent in these inventories.

The NADW equivalent thickness (Figure 5) exceeds 2000 m in much of the deeper main basins of the Atlantic, but exceeds 4000 m only in very small areas of the deepest parts of the North Atlantic. NADW thickness is reduced to the south, not exceeding 2000 m in many places south of the Atlantic at 30°S, and only nosing eastward south of Africa a short distance into the Indian Ocean (to 60°E) at values exceeding 1000 m. South of 40°S NADW is carried east in the ACC, keeping a core generally exceeding 500-m thickness in the ACC around the world. In addition, tongues of NADW equivalent thickness exceeding 500 m extend northward toward the equator in the Central Indian Basin, and northward into many of the deep Pacific Basins. NADW equivalent thicknesses exceeding 250 m are estimated throughout most of the deep basins of the Indian and Pacific Oceans.

In contrast to NADW, AABW exceeds 4000 m thickness over some of the Weddell and Enderby Abyssal Plains, and spreads northward from the Antarctic to fill the majority of the abyssal Indian and Pacific Oceans, with equivalent thicknesses (Figure 5) exceeding 1000 m, and often 2000 m, in all of the deep basins of these oceans. Even in the Brazil Basin of the South Atlantic, AABW equivalent thickness exceeding 1000 m extends northward to the equator. While thinning further northward, AABW equivalent thickness still exceeds 250 m until nearly 30°N in both basins of the North Atlantic.

The area integral of these equivalent thicknesses estimates the total fraction of NADW versus AABW in the sampled globe. However, because of the limited number of water masses, various bodies of salt water including the Arctic Ocean, the Mediterranean Sea, the Red Sea, the Persian Gulf, the Black Sea, the Caspian Sea, the Japan Sea, and the Sea of Okhotsk are excluded from the analysis because their seawater properties are

poorly spanned by the water-mass definitions (Table 3) used here. Before excluding these bodies, the ocean water volume encompassed by the portion of the gridded data set with all necessary seawater properties for the calculation is  $1.317 \times 10^9 \text{ km}^3$ . After excluding these bodies, it is  $1.293 \times 10^9 \text{ km}^3$ , a reduction of  $< 2\%$ . The estimated volume of NADW is  $0.268 \times 10^9 \text{ km}^3$  and that of AABW is  $0.468 \times 10^9 \text{ km}^3$ . By this estimate the amount of the global ocean analyzed here occupied by AABW is 36% and that by NADW 21%, summing to a total of 57%. The ratio of AABW to NADW is 1.74.

Bottom concentrations of NADW and AABW (Figure 6) reveal that AABW is predominant in contact with the ocean floor. High NADW bottom concentrations are limited to the North Atlantic, and the western boundary and Angola Basin in the South Atlantic. Elsewhere, the fraction of NADW generally exceeds 0.1, but does not reach 0.3 (except in Weddell, Enderby, and Australian-Antarctic Basins, where bottom concentrations of NADW are  $< 0.1$ ). Bottom AABW concentrations are dominant in all the deep basins of both hemispheres of the Indian and Pacific Oceans, and also dominate in the Cape, Argentine, and Brazil Basins of the South Atlantic. Small fractions of AABW even reach into the North Atlantic and the Angola Basin of the South Atlantic at the sea floor.

Area integrals of the bottom fractions of NADW and AABW quantify the extent to which these water masses cover the bottom of the sampled globe. Again, the Arctic Ocean and the marginal seas mentioned above are excluded from the analysis, as well any other areas where the fit residuals are large (as specified in Section 3) at the ocean floor. The area of the World Ocean floor is about  $0.361 \times 10^9 \text{ km}^2$ , but that in which the analysis is valid is only  $0.311 \times 10^9 \text{ km}^2$ , a reduction of nearly 14% (most of the

continental shelves do not contain valid solutions, and the marginal seas account for a larger fraction of the global ocean surface area than global ocean volume). Of this reduced area,  $0.180 \times 10^9 \text{ km}^2$  is effectively covered by AABW, and only  $0.081 \times 10^9 \text{ km}^2$  by NADW. By this estimate the amount of the global ocean floor analyzed here covered by AABW is 58% and that by NADW is 26%, summing to a total of 84%. The remainder is covered by the other water masses (primarily AAIW, especially in shallower regions). The ratio of AABW to NADW covering the ocean bottom analyzed here is 2.22.

## 6. Sensitivity studies

Two aspects of the sensitivity of the solution are analyzed here. First, the sensitivity of the results to changes in the seawater properties used is explored by varying those for two of the water masses used. Second, the effect of changing the weights accorded to conservation of each of the different seawater properties and mass conservation is quantified by systematically varying the variances assigned to each of these weights. For the purposes of brevity, the discussion is limited to the effect of these changes on the global volumes of AABW and NADW expressed as percentages of the global ocean volume (excluding the Arctic Ocean and marginal seas as previously detailed), and their ratio.

AABW is chosen as one of the water mass for which to vary seawater properties. This choice is made for several reasons. First, AABW is one of the two central water masses in this study, with NADW being the other. Second, while the model used here includes three components (LNADW, UNADW) to represent NADW, AABW is only afforded a single set of seawater properties (nominally those of WSBW). In reality,

AABW is formed in multiple locations, and each variety has different seawater properties. Finally, it is possible to choose “AABW” seawater properties to approximate those of one of its near-surface ventilated components, in an attempt to estimate the contribution of the ventilated component of this water mass to the global ocean volume.

While WSBW is the most extreme variety of AABW in terms of its cold temperature, Adélie Land Bottom Water (ALBW) is an intermediate variety. Here this water mass is characterized by the seawater properties of the coldest, densest AABW found in the deep Australian-Antarctic Basin. Similarly, Ross Sea Bottom Water (RSBW), the most moderate of the three varieties of AABW characterized here, is characterized by the seawater properties of the coldest, densest AABW over the Amundsen Abyssal Plain (Figure 1; Tables 2 and 3). The AABW seawater properties used, whether characteristic of WSBW, ALBW, or RSBW, are all relatively cold, fresh, with small negative PV values, and high in PO, NO, and deep SO when contrasted with the constituents of NADW (Table 3).

Characterizing the AABW seawater properties using those of ALBW instead of WSBW increases the AABW volume to 38% of the global sampled volume instead of 36%, with no change in the NADW percentage (Table 4). In this case the ratio of AABW volume to NADW volume increases to 1.80 from 1.74. Furthermore, when RSBW seawater properties are used to characterize AABW, the estimate of the percentage of AABW contributing to the global ocean volume increases to 41%, and the NADW percentage decreases to 17% from 21%, so that the AABW to NADW ratio increases to 2.44. Thus, use of increasingly less extreme AABW properties increasingly raises the estimate of AABW relative to NADW volume in the global ocean. In other

words, the use of WSBW in the standard calculations presented Section 5 likely de-emphasizes the role of AABW in filling the global ocean.

As mentioned previously, all varieties of AABW consist of dense waters formed near the surface of Antarctica that mix considerably with ambient waters on their path to the abyss. These dense surface waters may be diluted by about a factor of three on their descent of the continental slope [Orsi *et al.*, 1999]. Here one prominent near-surface contributor of AABW is referred to as the Weddell Shelf Water (WSW). The seawater properties of WSW are estimated from cold ( $\theta < -1.8^{\circ}\text{C}$ ) and shallow ( $P < 200$  dbar) waters in the western Weddell Sea (Figure 1; Tables 2 and 3). These WSW seawater properties can be used to characterize “AABW” in a more radical sensitivity experiment. This experiment can be thought of as an attempt to quantify the influence of this locally ventilated component of AABW through the global ocean.

Using the WSW seawater properties to characterize “AABW” results in a decrease of AABW volume in the global ocean to 23%, and a decrease of the volume of NADW to 17% (Table 4). The ratio of AABW to NADW in this instance is reduced to 1.33, a substantial decrease from the value of 1.74 when WSDW properties are used to characterize AABW. The entrainment process imparts additional characteristics to AABW, including some of those of NADW. These additional characteristics are excluded from the “AABW” by using WSW seawater properties. Thus, the decrease of “AABW” volume might be expected since the “AABW” properties solely approximate those of the ventilated water-mass in this calculation [Broecker *et al.*, 1998]. However, the “AABW” volume still exceeds the NADW volume in this sensitivity experiment.

While LSW is a directly ventilated component of NADW, it is more difficult to trace the directly ventilated components that make up ISOW and DSOW, so calculations estimating the influence of directly ventilated components of LNADW on global ocean NADW volumes are not attempted here.

Seawater properties of the ISOW component of NADW used in Section 5 are relatively steady in comparison to the LSW component [Yashayaev, 2007]. In the climatology (Table 3), LSW is relatively warm, salty, and high in PV compared with the most strongly ventilated year for LSW since at least 1928, which is 1994. While values for PO, NO, and SO are not readily available for 1994, Figure 8 of Yashayaev [2007] allows estimation of values of  $\theta$ , S, and PV for the 1994 vintage of LSW. These values, together with the climatological values of PO, NO, and SO for LSW used in Section 5, are referred to as LSW\_1994. Use of seawater properties of LSW\_1994 instead of those of the LSW in the climatology for UNADW in the model results in an increase in the AABW volume to 37% from 36%, while the NADW volume remains at 21% (Table 4). These small changes increase the ratio of AABW to NADW volumes to 1.77 from 1.74. These results suggest that the global results here are relatively insensitive to the vintage of LSW used in the calculation.

The seven weights given to the variances of the six seawater water properties and mass conservation are carefully chosen, but those choices are certainly subjective. To explore the sensitivity of the solutions to variations in those weights, volume estimates of AABW and NADW are made with each of the seven individual variances for the weights either doubled or halved while the rest of the variances were kept constant. This procedure results in 14 estimates. The AABW and NADW volumes expressed as

percentages of the global ocean volume sampled vary by standard deviations of  $\pm 0.4\%$ , and  $\pm 0.3\%$ , respectively. The ratios of AABW to NADW volumes for these 14 estimates vary by a standard deviation of 0.04 around a central value of 1.75. Larger variations in the variances of the weights, or varying several weights together, would have a larger impact on the solution.

## 7. Discussion

The sensitivity experiments detailed above suggest that small changes in the weights or the seawater properties of one or more of the water masses chosen should not have a qualitative effect on the solution. Experimentation with variations in water mass choices and seawater properties beyond those discussed here suggest that the ratio of AABW to NADW volume in the global ocean is not likely to be exactly 1.74, or even 1.7. However, it is almost certainly more than 1 and less than 3. One might appropriately think of AABW occupying about twice the volume of NADW.

However, a wholesale change in selection of one or more of the water masses could have a much bigger impact on the solution than the sensitivity experiments presented. For instance, Circumpolar Deep Water (CDW) is not included in this analysis, because it originates neither from ventilation nor introduction from a marginal sea, but from mixing of abyssal, deep, and intermediate water masses, including AABW and NADW. CDW, if included in the analysis, would contain significant amounts of AABW and NADW and obscure the relative contributions of these ventilated water masses to the global total below the thermocline.

The branches of the deep global meridional overturning circulation associated with NADW and AABW are similar in size,  $\sim 17 \times 10^6 \text{ m}^3 \text{ s}^{-1}$  each, based on physical inverse models [Ganachaud, 2003; Lumpkin and Speer, 2007] as well as tracer budgets and assimilations [Broecker *et al.*, 1998; Peacock *et al.*, 2000; Orsi *et al.*, 2002; Schlitzer, 2007]. The volume of AABW is estimated here to be about 1.7 times that of NADW (AABW volume is still about 1.3 times that of NADW even if only the locally ventilated component of AABW is considered). These results reinforce the importance of the Antarctic limb of the global deep meridional overturning circulation. These overturning rates and volumes suggest an  $\sim 870$ -year global average residence time for AABW and an  $\sim 500$ -year time for NADW.

Being colder and denser than NADW, AABW fills the bulk of the abyss [Orsi *et al.*, 2001]. The ratio of AABW to NADW in contact with the deep ocean floor is estimated here to be over 2. Mixing tends to be stronger over rough topography, especially in the Southern Ocean [Naviera Garabato *et al.*, 2004], as well as just downstream of deep overflows at sills between deep basins [Roemmich *et al.*, 1996], making AABW more likely to be subject to strong mixing than NADW. This idea is supported by inverse estimates of much stronger diffusivities in density range for AABW than NADW [Lumpkin and Speer, 2007].

Both NADW [Yashayaev, 2007] and AABW [Fahrbach *et al.*, 2004; Rintoul, 2007] components vary over interannual and longer timescales. NADW variations can be traced at least as far as the equator in the Atlantic Ocean with a time-scale of about 20 years [Fine *et al.*, 2002]. AABW variability has been observed at least as far as the equator in the Atlantic [Andri  *et al.*, 2003], and as far as  $47^\circ\text{N}$  in the Pacific [Fukasawa

483 *et al.*, 2004]. While a steady-state approach has been taken in the analysis here, none of  
484 the variations in NADW and AABW seawater properties are likely to be so large that  
485 they would have a first-order impact on the results presented here because AABW and  
486 NADW have very different properties in comparison to their observed temporal  
487 variations. This statement is supported by the sensitivity calculation presented in Section  
488 6 that substitutes 1994 values of  $\theta$ ,  $S$ , and PV of LSW for the UNADW values of those  
489 seawater properties found in the climatology.

490       However, observed deep temperature changes in the North Atlantic are reported to  
491 make a small but significant (order 10%) contribution to variations in the global heat  
492 budget [*Levitus et al.*, 2005]. While observed changes in the AABW are neither  
493 especially large, nor as closely observed as those in the North Atlantic, they do appear to  
494 occur in a thick abyssal layer and extend over a large fraction of the ocean floor in the  
495 South Atlantic [*Johnson and Doney*, 2006] and throughout the Pacific [*Johnson et al.*,  
496 2007], and so may also contribute to global heat budget changes at a similar magnitude.  
497 Observing variations in both limbs of the global meridional overturning circulation  
498 appears to be important for the study of global climate.

**Acknowledgments:** The NOAA Office of Oceanic and Atmospheric Research and the NOAA Climate Program Office further supported GCJ. This analysis was made possible by all the hard work put in by World Ocean Circulation Experiment (WOCE) scientists to collect high-quality oceanographic data and that of *Gouretski and Koltermann* [2004] to quality control and grid the WOCE and other historical data sets. Figure color palettes are from [www.colorbrewer.org](http://www.colorbrewer.org), by Cynthia A. Brewer, Penn State. John Lyman, John Bullister, Alex Orsi, and LuAnne Thompson all helped this research along with discussions. Three anonymous reviewers and the journal editor also provided critiques that substantially improved the results. The findings and conclusions in this article are those of the author and do not necessarily represent the views of the National Oceanic and Atmospheric Administration. This is Pacific Marine Environmental Laboratory contribution number 3102.

## Reference List

- Anderson, L. A., and J. L. Sarmiento (1994), Redfield ratios of remineralization determined by nutrient data analysis, *Global Biogeochem. Cycles*, 8, 65–80.
- Andri , C., Y. Gouriou, B. Bourl s, J.-F. Termon, E. S. Braga, P. Morin, and C. Oudot (2003), Variability of AABW properties in the equatorial channel at 35 W, *Geophys. Res. Lett.*, 30, 8007, doi:10.1029/2002GL015766.
- Beal, L. M., A. Ffield, and A. L. Gordon (2000), Spreading of Red Sea overflow waters in the Indian Ocean, *J. Geophys. Res.*, 105, 8549–8564.
- Broecker, W. S. (1974), "NO", a conservative water-mass tracer, *Earth Planet. Sci. Lett.*, 23, 100–107.
- Broecker, W. S., S. L. Peacock, S. Walker, R. Weiss, E. Fahrbach, M. Schroeder, U. Mikolajewicz, C. Heinze, R. Key, T.-H. Peng, and S. Rubin (1998), How much deep water is formed in the Southern Ocean?, *J. Geophys. Res.*, 103, 15,833–15,843.
- Dickson, R. R., and J. Brown (1994), The production of North Atlantic Deep Water: Sources, rates, and pathways, *J. Geophys. Res.*, 99, 12,319–12,342.
- Fahrbach, E., M. Hoppema, G. Rohardt, M. Schr der, and A. Wisotzki (2004), Decadal-scale variations of water mass properties in the deep Weddell Sea, *Ocean Dyn.*, 54, 77–91, doi:10.1007/s10236-003-0082-3.
- Fine, R. A., M. Rhein, and C. Andri  (2002), Using and CFC effective age to estimate propagation and storage of climate anomalies in the deep western North Atlantic Ocean, *Geophys. Res. Lett.*, 29, 2227, doi:10.1029/2002GL015618.

533 Foster, T. D., and E. C. Carmack (1976), Frontal zone mixing and Antarctic Bottom  
 534 Water formation in the southern Weddell Sea, *Deep-Sea Res.*, *23*, 301–307.  
 535 Fukasawa, M., H. Freeland, R. Perkin, T. Watanabe, H. Uchida, and A. Nishina (2004),  
 536 Bottom water warming in the North Pacific Ocean, *Nature*, *427*, 825–827.  
 537 Ganachaud, A. (2003), Large-scale mass transports, water mass formation, and  
 538 diffusivities estimated from World Ocean Circulation Experiment (WOCE)  
 539 hydrographic data, *J. Geophys. Res.*, *108*, 3213, doi:10.1029/2002JC001565.  
 540 Gouretski, V. V., and K. P. Koltermann (2004), WOCE Global Hydrographic  
 541 Climatology, *Berichte des Bundesamtes für Seeschifffahrt und Hydrographie*, *35*,  
 542 pp. 52 + 2 CD-ROMs.  
 543 Harvey, J., and M. Arhan (1988), The water masses of the central North Atlantic in  
 544 1983–84, *J. Phys. Oceanogr.*, *18*, 1855–1875.  
 545 Johnson, G. C., and S. C. Doney (2006), Recent western South Atlantic bottom water  
 546 warming, *Geophys. Res. Lett.*, *33*, L14614, doi:10.1029/2006GL026769.  
 547 Johnson, G. C., S. Mecking, B. M. Sloyan, and S. E. Wijffels (2007), Recent bottom  
 548 water warming in the Pacific Ocean, *J. Climate*, *20*, 5365–5375.  
 549 Levitus, S., J. Antonov, and T. Boyer (2005), Warming of the world ocean, 1955–2003,  
 550 *Geophys. Res. Lett.*, *32*, L02604, doi:10.1029/2004GL01592.  
 551 Lumpkin, R., and K. Speer (2007), Global Ocean meridional overturning, *J. Phys.*  
 552 *Oceanogr.*, *37*, 2550–2562.  
 553 Mantyla, A. W., and J. L. Reid (1983), Abyssal characteristics of the World Ocean  
 554 waters, *Deep-Sea Res., Part A*, *30*, 805–833.

555 McCartney, M. S. (1977), Subantarctic Mode Water, in *A Voyage of Discovery, George*  
 556 *Deacon 70<sup>th</sup> Anniversary Volume*, edited by M. Angel, Pergamon Press, Oxford,  
 557 pp. 103–119.

558 Naviera Garabato, A. C., K. L. Polzin, B. A. King, K. J. Heywood, and M. Visbeck  
 559 (2004), Widespread intense turbulent mixing in the Southern Ocean, *Science*, *303*,  
 560 210–213, doi:10.1126/science.1090929.

561 Orsi, A. H., S. S. Jacobs, A. L. Gordon, and M. Visbeck (2001), Cooling and ventilating  
 562 the abyssal ocean, *Geophys. Res. Lett.*, *28*, 2923–2926.

563 Orsi, A. H., G. C. Johnson, and J. L. Bullister (1999), Circulation, mixing, and production  
 564 of Antarctic Bottom Water, *Prog. Oceanogr.*, *43*, 55–109.

565 Orsi, A. H., W. J. Smethie, Jr., and J. L. Bullister (2002), On the total input of Antarctic  
 566 waters to the deep ocean: A preliminary estimate from chlorofluorocarbon  
 567 measurements, *J. Geophys. Res.*, *107*, 3122, doi:10.1029/2001JC000976.

568 Peacock, S., M. Visbeck, and W. Broecker (2000), Deep water formation rates from  
 569 global tracer distributions: An inverse approach, in *Inverse Methods in Global*  
 570 *Biogeochemical Cycles*, *AGU Monograph 114*, edited by P. Kasibhatla, M.  
 571 Heimann, P. Rayner, N. Mahowald, R. Prinn, and D. Hartley, AGU, Washington,  
 572 D. C., pp. 185–195.

573 Pedlosky, J. (1987), *Geophysical Fluid Dynamics*, 2<sup>nd</sup> ed., 710 pp., Springer, New York.

574 Poole, R., and M. Tomczak (1999), Optimum multiparameter analysis of the water mass  
 575 structure in the Atlantic Ocean thermocline. *Deep-Sea Res. I*, *46*, 1895–1921.

576 Reid, J. L., and R. J. Lynn (1971), On the influence of Norwegian-Greenland and  
 577 Weddell seas on the bottom waters of the Indian and Pacific Oceans, *Deep-Sea*  
 578 *Res.*, *18*, 1063–1088.

579 Rintoul, S. R. (2007), Rapid freshening of Antarctic Bottom Water formed in the Indian  
 580 and Pacific Oceans, *Geophys. Res. Lett.*, *34*, L06606, doi:10.1029/2006GL028550.

581 Roemmich, D., S. Hautala, and D. Rudnick (1996), Northward abyssal transport through  
 582 the Samoan Passage and adjacent regions, *J. Geophys. Res.*, *101*, 14,039–14,055.

583 Sarmiento, J. L., J. Simeon, A. Gnanadesikan, N. Gruber, R. M. Key, and R. Schlitzer,  
 584 (2007), Deep ocean biogeochemistry of silicic acid and nitrate, *Global*  
 585 *Biogeochem. Cycles*, *21*, GB1S90, doi: 10.1029/2005GB002720.

586 Schlitzer, R. (2007), Assimilation of radiocarbon and chlorofluorocarbon data to  
 587 constrain deep and bottom water transports in the World Ocean, *J. Phys.*  
 588 *Oceanogr.*, *37*, 259–276.

589 Talley, L. D. (1993), Distribution and formation of North Pacific Intermediate Water, *J.*  
 590 *Phys. Oceanogr.*, *23*, 517–537.

591 Talley, L. D., and M. S. McCartney (1982), Distribution and circulation of Labrador Sea  
 592 Water, *J. Phys. Oceanogr.*, *12*, 1189–1205.

593 Tomczak, M., and D. G. B. Large (1989), Optimum multiparameter analysis of mixing in  
 594 the thermocline of the eastern Indian Ocean, *J. Geophys. Res.*, *94*, 16,141–16,149.

595 Tsuchiya, M., L. D. Talley, and M. S. McCartney (1992), An Eastern Atlantic section  
 596 from Iceland southward across the equator, *Deep-Sea Res. A*, *39*, 1885–1917.

597 Warren, B. A. (1981), Deep Circulation of the World Ocean, in *Evolution of Physical*  
598 *Oceanography*, edited by B. A. Warren and C. Wunsch, pp. 6–41, The MIT Press,  
599 Cambridge, Massachusetts.

600 Yashayaev, I. (2007), Hydrographic changes in the Labrador Sea, 1960–2005, *Prog.*  
601 *Oceanogr.*, 73, 242–276.

602

602 Table 1. Abbreviations and full names of water masses listed from densest to lightest  
603 above the upper dividing line. When applicable, alternate abbreviations and names are  
604 listed below the relevant water mass. For Section 6 sensitivity experiments ALBW,  
605 RSBW, and even WSW are substituted for AABW (between upper and lower dividing  
606 lines) and LSW\_1994 is substituted for UNADW (below lower dividing line).

Abbreviation	Full Water Mass Name
(Alternate)	(Alternate)
AABW	Antarctic Bottom Water
(WSBW)	(Weddel Sea Bottom Water)
LNADW	Lower North Atlantic Deep Water
(ISOW)	(Iceland-Scotland Overflow Water)
UNADW	Upper North Atlantic Deep Water
(LSW)	(Labrador Sea Water)
MSOW	Mediterranean Sea Overflow Water
RSOW	Ross Sea Overflow Water
AAIW	Antarctic Intermediate Water
NPIW	North Pacific Intermediate Water
ALBW	Adélie Land Bottom Water
RSBW	Ross Sea Bottom Water
WSW	Weddell Shelf Water
LSW_1994	1994 LSW*

607 \*Values of  $\theta$ , S, and PV adopted from *Yashayaev* [2007], see his Figure 8.

608 Table 2. Locations (Figure 1) and potential densities ( $\sigma_\theta$ ) around which seawater  
609 properties (Table 3) are estimated for each water mass (Table 1), from densest to lightest  
610 (above upper dividing line). For Section 6 sensitivity experiments ALBW, RSBW, and  
611 even WSW properties (Table 3) are substituted for those of AABW (between upper and  
612 lower dividing lines) and LSW\_1994 properties are substituted for those of UNADW  
613 (below lower dividing line).

Water Mass	Latitude	Longitude	$\sigma_\theta$ [kg m <sup>-3</sup> ]
AABW	67°S	30°W	bottom*
LNADW	58°N	50°W	bottom*
UNADW	58°N	50°W	27.77
MSOW	40°N	15°W	27.7
RSOW	15°N	55°E	27.3
AAIW	55°S	85°W	27.1
NPIW	37°N	160°E	26.8
ALBW	60°S	122°E	bottom*
RSBW	72°S	165°W	bottom*
WSW	68°S	53°W	surface**
LSW_1994***	Labrador Sea at $\sigma_2 = 36.94$ kg m <sup>-3</sup>		

614 \* Seawater properties estimated from coldest densest (bottom) values

615 \*\* Seawater properties estimated from cold ( $\theta < -1.8^\circ\text{C}$ ) shallow ( $P < 100$  dbar) values

616 \*\*\* Values of  $\theta$ ,  $S$ , and  $PV$  adopted from *Yashayaev* [2007], see his Figure 8.

617 Table 3. Seawater properties estimated at various locations and density or depth horizons  
618 (Table 2) for each water mass (Table 1) used in the primary calculations (above the upper  
619 dividing line). For Section 6 sensitivity experiments ALBW, RSBW, and even WSW  
620 properties are substituted for those of AABW (between upper and lower dividing lines)  
621 and LSW\_1994 properties are substituted for those of UNADW (below lower dividing  
622 line).

Water	$\theta$	S	PO*	NO**	SO***	PV
Mass	[°C]	[PSS-78]	[ $\mu\text{mol kg}^{-1}$ ]	[ $\mu\text{mol kg}^{-1}$ ]	[ $\mu\text{mol kg}^{-1}$ ]	[ $10^{-12} \text{ m}^{-1} \text{ s}^{-1}$ ]
AABW	-0.88	34.641	638	595	456	-3.7
LNADW	1.30	34.878	466	451	313	24
UNADW	3.32	34.894	476	465	302	5.6
MSOW	11.27	36.244	347	349	202	55
RSOW	12.05	35.897	452	353	101	41
AAIW	4.64	34.227	572	544	286	-52
NPIW	5.68	34.000	495	454	251	162
ALBW	-0.55	34.678	632	599	436	-11
RSBW	-0.24	34.702	618	580	418	-8
WSW	-1.85	34.246	659	574	446	-160
LSW_1994	2.71	34.831	475	464	301	2.1

623 \*PO =  $170[\text{PO}_4] + [\text{O}_2]$ .

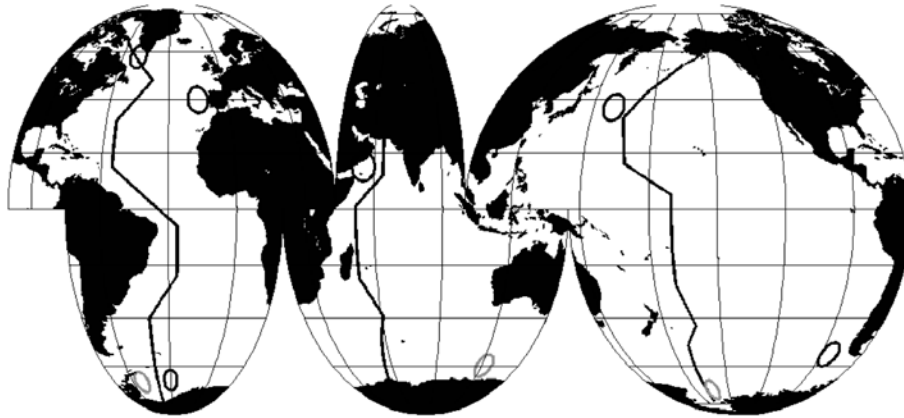
624 \*\*NO =  $10.625[\text{NO}_3] + [\text{O}_2]$ .

625 \*\*\*SO =  $1.66[\text{H}_4\text{SiO}_4] + [\text{O}_2]$ ,

626 Table 4. Estimated volumes of AABW and NADW expressed as a percentage of the  
627 sampled global ocean volume in the WOCE Global Hydrographic Climatology  
628 [*Gouretski and Koltermann*, 2004] excluding the Arctic Ocean and marginal seas as  
629 mentioned in the text ( $1.29 \times 10^9 \text{ km}^3$ ), along with the ratio of the volumes (above upper  
630 dividing line). For Section 6 sensitivity experiments ALBW, RSBW, and even WSW  
631 properties (Table 3) are substituted for those of AABW (between upper and lower  
632 dividing lines) and LSW\_1994 properties are substituted for those of UNADW (below  
633 lower dividing line).

AABW	UNADW	AABW	NADW	AABW/NADW
Variety	Variety	Volume [%]	Volume [%]	Volume Ratio
WSBW	LSW	36	21	1.74
ALBW	LSW	38	21	1.80
RSBW	LSW	41	17	2.44
WSW*	LSW	23	17	1.33
WSBW	LSW_1994	37	21	1.77

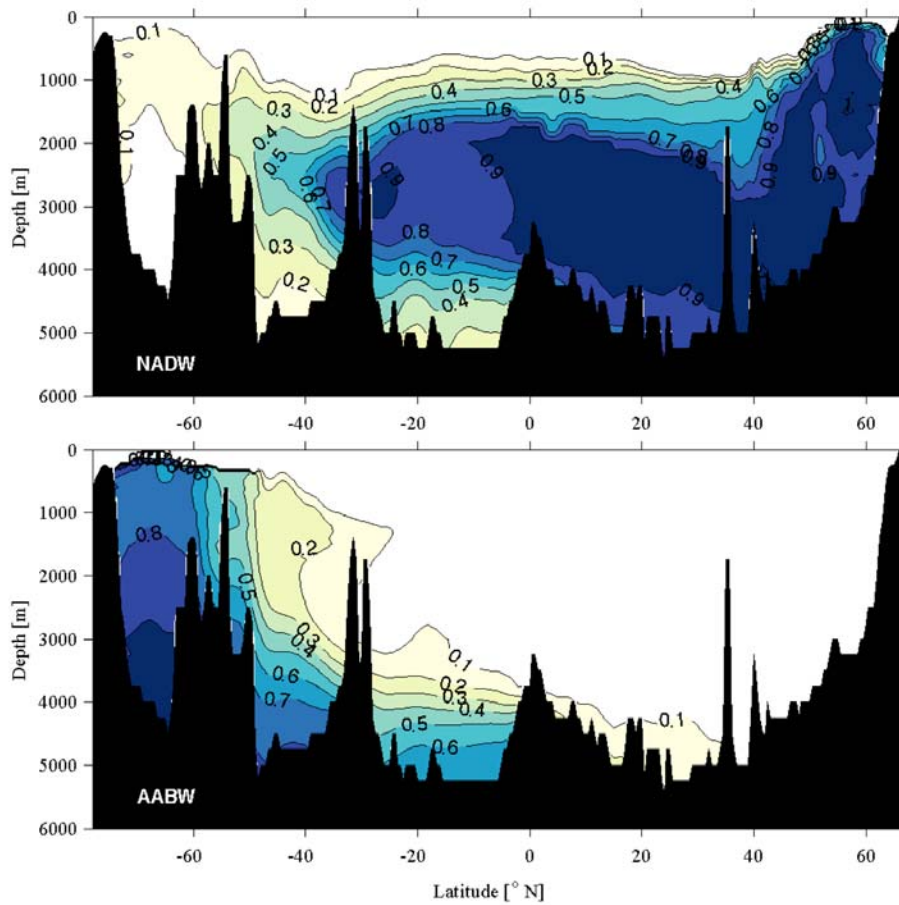
634 \*Near-surface ventilated component of AABW



635

636 Figure 1. Locations of quasi-meridional sections (solid lines) running through the deep  
 637 western basins of each of the three major oceans (solid lines) for the Atlantic (Figure 2),  
 638 the Indian (Figure 3) and the Pacific (Figure 4) Oceans on an interrupted Mollweide  
 639 projection. Also, locations (black outlined ellipses; above the upper dividing line in all  
 640 tables) at which seawater properties for the water masses used in this study are estimated.  
 641 Alternate locations for AABW property estimates (grey outlined ellipses; between the  
 642 dividing lines in all tables) are also shown.

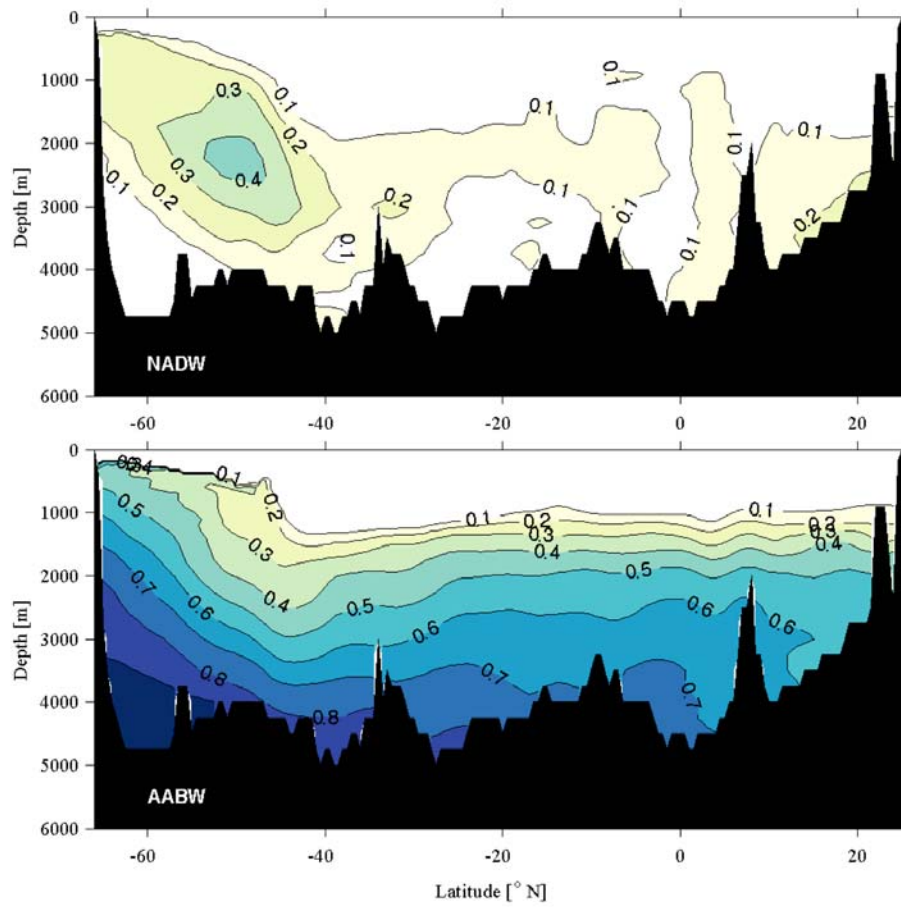
643



643

644 Figure 2. Fraction of NADW = LNDW + UNADW (upper panel) and AABW =  
 645 WSBW (lower panel) for a quasi-meridional section through the western basins of the  
 646 Atlantic Ocean (Figure 1) contoured (with values increasing from light yellow to dark  
 647 blue) at 0.1 intervals as a function of depth and latitude. Bathymetry is shaded black.

648

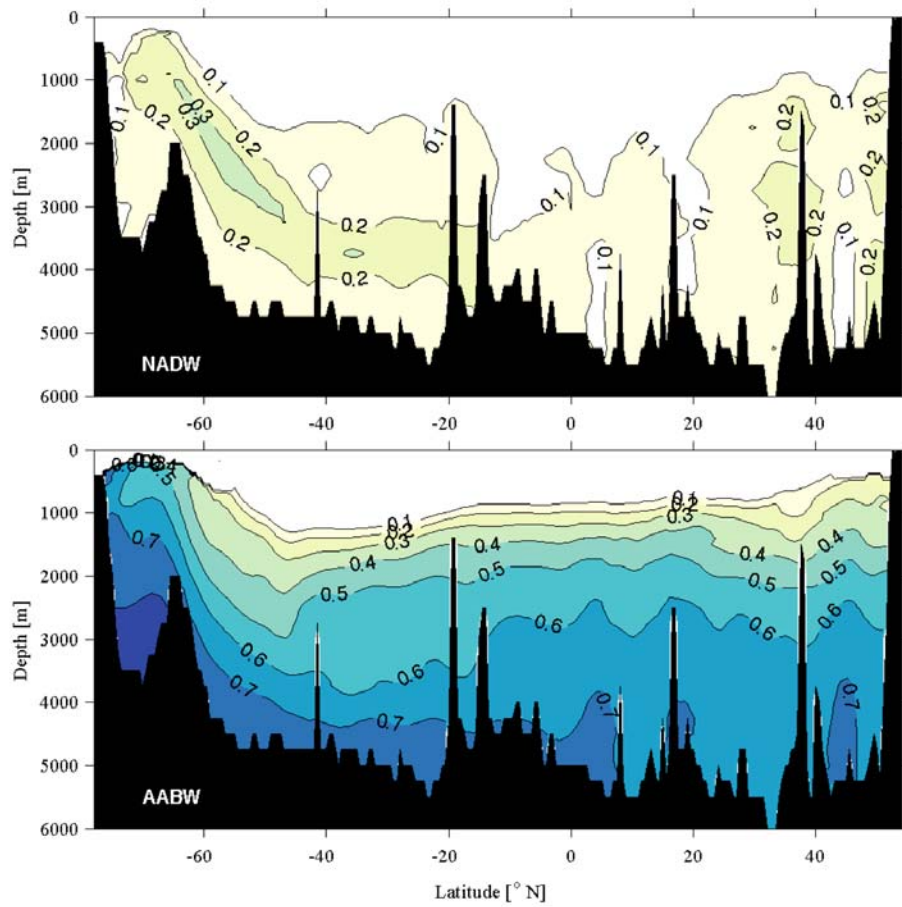


648

649 Figure 3. Following Figure 2, but for a quasi-meridional section through the western

650 basins of the Indian Ocean (Figure 1).

651

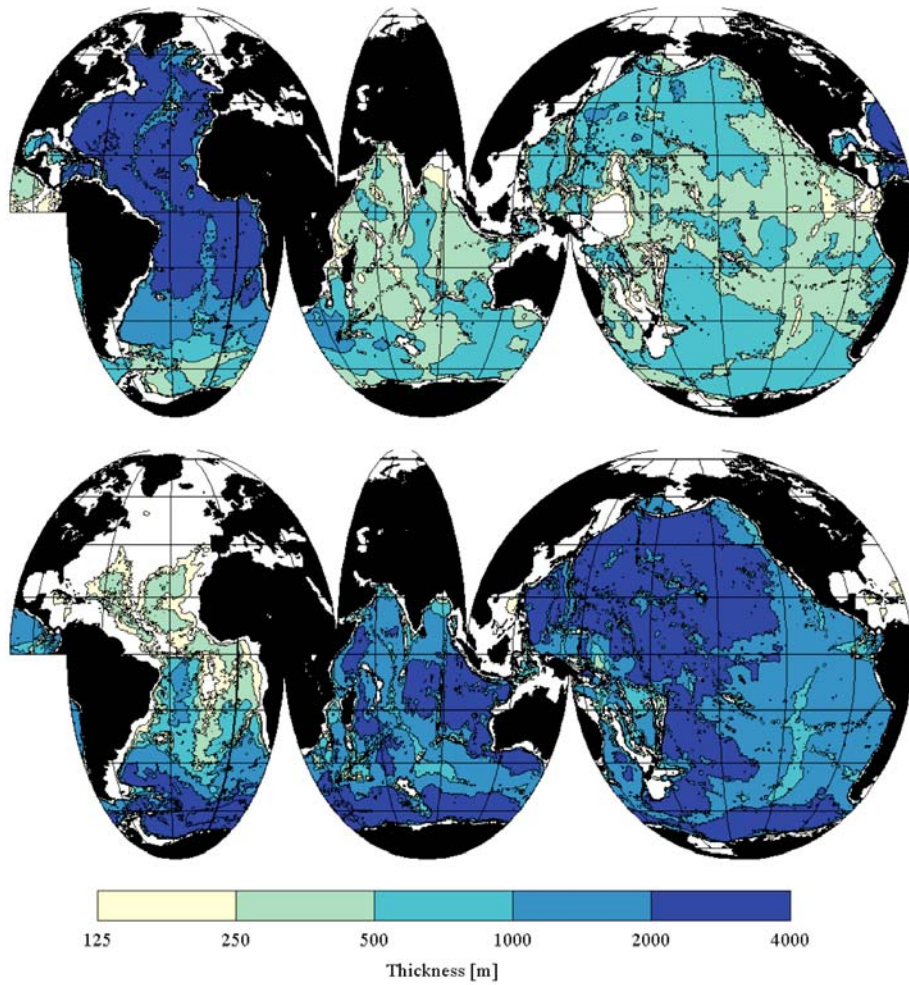


651

652 Figure 4. Following Figure 3, but for a quasi-meridional section through the western

653 basins of the Pacific Ocean (Figure 1).

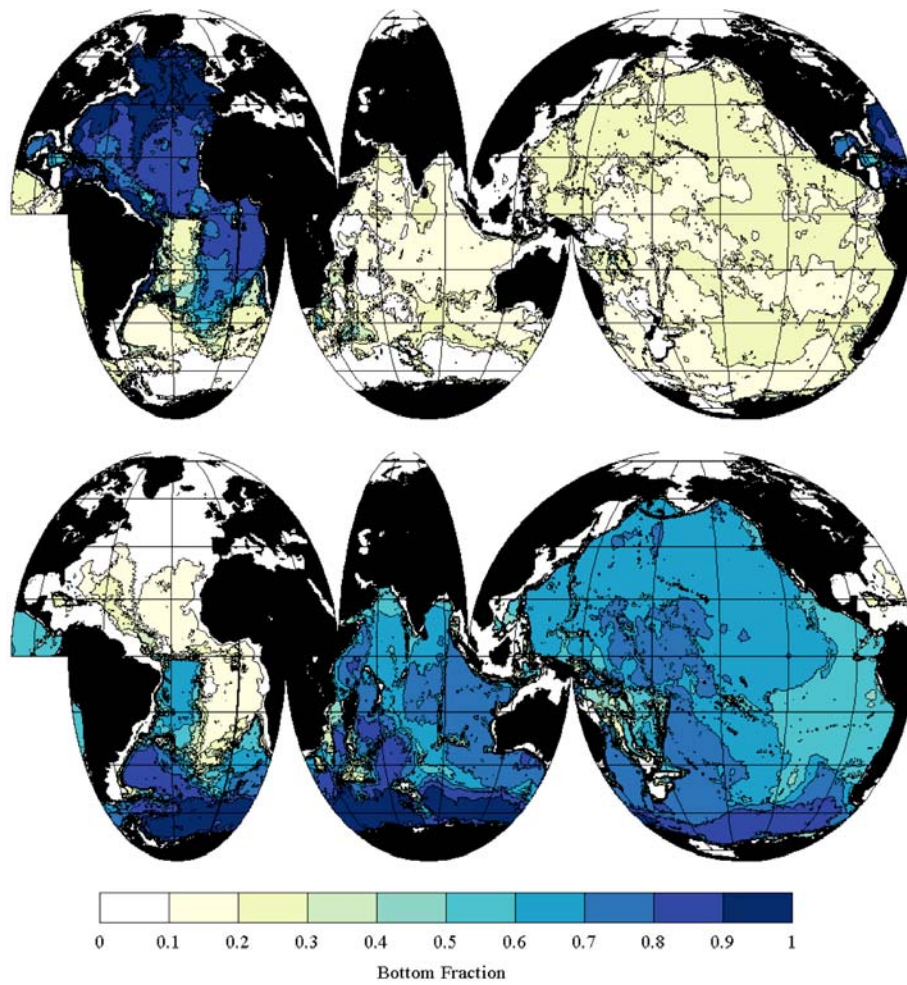
654



654

655 Figure 5. Depth-integral of fraction of NADW = LNADW + UNADW (upper panel)  
 656 and AABW = WSBW (lower panel) contoured (color bar) at doubling intervals from 125  
 657 to 4000 m. The small areas with values exceeding 4000 m are contoured, but not  
 658 distinguished by a change in color from those with values exceeding 2000 m.

659



659

660 Figure 6. Fraction of NADW = LNDW + UNADW (upper panel) and AABW =  
 661 WSBW (lower panel) at the deepest sample in the climatology contoured (colorbar) at 0.1  
 662 intervals.

663

Auxiliary Material Submission for Paper 2007JC004477

Quantifying Antarctic Bottom Water and North Atlantic Deep Water Volumes.

Gregory C. Johnson

(NOAA/Pacific Marine Environmental Laboratory, Seattle)

J. Geophys. Res., 113, doi:10.1029/2007JC004477, 2008

## Introduction

The auxiliary material for paper 2007JC004477 consists of 3 tiff figures of quasi-meridional sections in the western basins of each of the three oceans (Atlantic, Indian, and Pacific) presenting fractions of the four water masses (NPIW, AAIW, RSOW, and MSOW). See Figure 1 of the article for the section locations. The solutions for these water masses are only valid for part of their domain, since the analysis is focused on the deep ocean, below the permanent pycnocline. Water mass fractions in areas where the solution is invalid as described in Section 3 of the article (mostly at or shallower than 1200 dbar) are set to zero in the figures.

Because only a limited number of water masses are used to span the seawater property space, sometimes a significant fraction of a water mass appears outside its expected geographical range. For instance, a small amount of spurious NPIW erroneously appears at the base of the pycnocline of the North Atlantic Ocean, as does RSOW in both the tropical Atlantic and tropical Pacific Oceans. However, for the most part, the water-mass distributions in these sections appear reasonable:

MSOW is found almost exclusively in the North Atlantic Ocean. The highest concentrations of RSOW spread southward from the North Indian Ocean. The highest concentrations of NPIW spread southward from North Pacific Ocean. Also, AAIW ventilates the base of the permanent pycnocline from the south and spreads northward in all three oceans.

The figure captions associated with each of these files are below.

1. 2007JC004477-fs01.tif: Fraction of (from top to bottom) NPIW, AAIW, RSOW, and MSOW for a quasi-meridional section through the western basins of the Atlantic Ocean contoured (with values increasing from light yellow to dark blue) at 0.1 intervals as a function of depth and latitude. Bathymetry is shaded black.

2. 2007JC004477-fs02.tif: Fraction of (from top to bottom) NPIW, AAIW, RSOW, and MSOW for a quasi-meridional section through the western basins of the Indian Ocean contoured (with values increasing from light yellow to dark blue) at 0.1 intervals as a function of depth and latitude. Bathymetry is shaded black.

3. 2007JC004477-fs03.tif: Fraction of (from top to bottom) NPIW, AAIW, RSOW, and MSOW for a quasi-meridional section through the western basins of the Pacific Ocean contoured (with values increasing from light yellow to dark blue) at 0.1 intervals as a function of depth and latitude. Bathymetry is shaded black.

